Article

Synthesis and Evaluation of a Library of Tri-Functional Scaffold-Derived Compounds as Modulators of the Insulin Receptor

Benjamin Fabre, Jan Picha, Vaclav Vanek, Irena Selicharová, Martina Chrudinová, Michaela Collinsova, Lenka Zakova, Miloš Bud#šínský, and Jiri Jiracek

ACS Comb. Sci., **Just Accepted Manuscript** • DOI: 10.1021/acscombsci.6b00132 • Publication Date (Web): 02 Nov 2016

Synthesis and Evaluation of a Library of Tri-Functional Scaffold-Derived Compounds as Modulators of the Insulin Receptor

Benjamin Fabre[1], Jan Pícha[1], Václav Vaněk, Irena Selicharová, Martina Chrudinová, Michaela Collinsová, Lenka Žáková, Miloš Buděšínský and Jiří Jiráček*

Institute of Organic Chemistry and Biochemistry, Czech Academy of Sciences, Flemingovo n. 2, 16610 Praha 6, Czech Republic

[1] *These authors contributed equally to this work*

Supporting Information

ABSTRACT: We designed a combinatorial library of tri-functional scaffold-derived compounds, which were derivatized with 30 different in-house-made azides. The compounds were proposed to mimic insulin receptor (IR)-binding epitopes in the insulin molecule and bind to and activate this receptor. This work has enabled us to test our synthetic and biological methodology and to prove its robustness and reliability for the solid-phase synthesis and testing of combinatorial libraries of the tri-functional scaffold-derived compounds. Our effort resulted in the discovery of two compounds, which were able to weakly induce the autophosphorylation of IR and weakly bind to this receptor at a 0.1 mM concentration. Despite these modest biological results, which well document the well-known difficulty in modulating protein-protein interactions, this study represents a unique example of targeting the IR with a set of non-peptide compounds that were specifically designed and synthesized for this purpose. We believe that this work can open new perspectives for the development of next-generation insulin mimetics based on the scaffold structure.

INTRODUCTION

Although promising, the modulation of protein-protein interactions (PPIs) has been recognized as one of the most challenging tasks in drug discovery.[1-4] Individual proteins involved in PPIs are, in many cases, thought to be undruggable, as the interfacial surface area formed by interacting proteins is usually large and solvent-exposed, the interaction surfaces are often shallow and featureless and the binding regions in protein-protein interactions are mostly non-contiguous.[5,6] For these reasons, it is difficult to mimic these interfaces by using small organic molecules. However, it can be assumed that molecules that mimic several different non-contiguous binding hotspots at the target protein surface have better chances of being potent modulators of protein functions than do compounds that mimic only one epitope.[7-9] For this purpose, we have recently developed a versatile tri-functional scaffold with orthogonally protected arms that can be selectively functionalized by different azides[10] (**I**, Fig. 1).

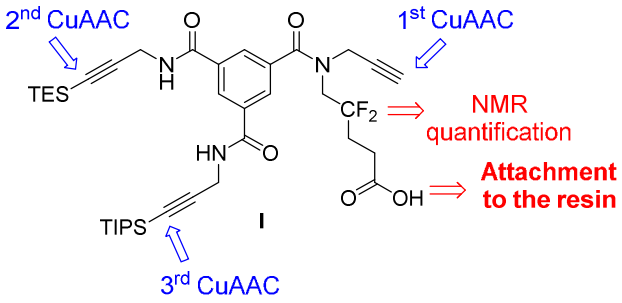

Figure 1. Tri-functional and orthogonally protected scaffold **I** (Ref.[10]). The three arms with free, TES-protected, and TIPS-protected propargylamine moieties enable successive copper(I)-catalyzed azide–alkyne cycloadditions (CuAACs). The spacer with carboxylic acid enables the attachment to the resin, and the CF_2 groups permit the quantitative ^{19}F NMR analysis.

Decades of intensive research did not fully clarify the main questions about the interaction of insulin with its transmembrane tyrosine kinase receptor, the insulin receptor (IR). Formidable problems with the production of IR constructs for structural studies and the complexity of IR-insulin interactions hampered the progress in deciphering the molecular nature of this assembly.[11] For more than a decade, our laboratory has been involved in the development of insulin

analogues to study the interaction of insulin with IR.[12-21] Recently, we contributed an important scientific result,[22] which provided the first insight into the nature of the insulin interaction with its primary binding site (Site 1) on the IR. The study was later followed by the elucidation of the IR-bound conformation of the crucial C-terminus of the insulin B-chain.[23,24] Although these studies were extremely important in insulin research, they did not provide information about the insulin interaction with its second binding site (Site 2) on the IR, which is thought to trigger IR-induced intracellular signaling. Nevertheless, extensive mutagenesis studies (reviewed in Ref.[25]) have identified key amino acids (GlyA1, IleA2, ValA3, GluA4, TyrA19, AsnA21, GlyB8, SerB9, LeuB11, ValB12, LeuB15, TyrB16, PheB24, PheB25 and TyrB26 for Site 1 and ThrA8, Ile A10, SerA12, LeuA13, GluA17, HisB10, GluB13 and LeuB17 for Site 2), which participate in the formation of binding epitopes (hotspots) in the insulin molecule that are responsible for binding to both IR sites.

Considering the central position of insulin in anti-diabetes therapy, there is a need for alternative forms of this hormone that would be metabolically stable, i.e., suitable for oral delivery, and less expensive to produce than insulin. Such medicines would have an impact on the cost-effectiveness of the health systems. Therefore, non-peptide molecules, such as insulin mimetics, which are able to bind efficiently IR and elicit the metabolic responses of native insulin (insulin agonists), would be of major interest. There are only a few reports on the development of non-peptide insulin mimetics. The majority of compounds with insulin agonist-like properties does not interact with the insulin-binding domain of IR but does interact with different intracellular targets (e.g., the Merck fungal metabolite L-783,281, Ref.[26]). Moreover, only a few compounds target the extracellular domain of IR, although this occurs with only a relatively weak affinity.[27-30] The most advanced progress in the development of insulin mimetics resulted from the application of phage display to generate peptides that are able to compete with insulin and have high affinities. However, these artificial peptides have a similar molecular weight to insulin and a similar stability. Nevertheless, the Novo Nordisk study[31-33] proved that the idea of insulin mimetics is realistic and promising. Moreover, a recent interesting study describes the discovery of an agonistic aptamer that is able to bind the IR (the interaction site is unknown), stimulate IR autophosphorylation and elicit the biological effects of native insulin.[34]

The incomplete structural information about the molecular nature of the insulin-IR interaction and the dynamic complexity of this interaction impede the efficient use of

computational techniques to predict the structures of artificial IR binders. However, we believe that molecules mimicking several different non-contiguous binding hotspots at the insulin surface have better chances of being potent insulin agonists than do compounds that only mimic one epitope. Moreover, we believe that a combinatorial approach for synthesizing and testing thousands of different compounds is the best starting strategy for the discovery of the first IR binders, which can be further optimized by molecular modeling and approaches analyzing the structure-function relationship. We hypothesized that a library of compounds derived from the structure of scaffold **I** could provide some new IR binders. Figure 2 explains the principle of our strategy using an example of a few residues forming binding epitopes in insulin. Recently, we showed[10] that a model compound derived from scaffold **I** can adopt an extended conformation and that the distances between the distal carbon atoms are similar to the size of insulin molecule (20-30 Å). Based on these presumptions, in this study, we employed scaffold **I** to generate a combinatorial library of 1,000 compounds using a pool of 30 different azides, which should provide various chemical properties. The library of the scaffold-**I**-derived compounds was tested for binding to isoform A of the insulin receptor (IR-A) and the IGF-1 receptor (IGF-1R) and its ability to activate these receptors.

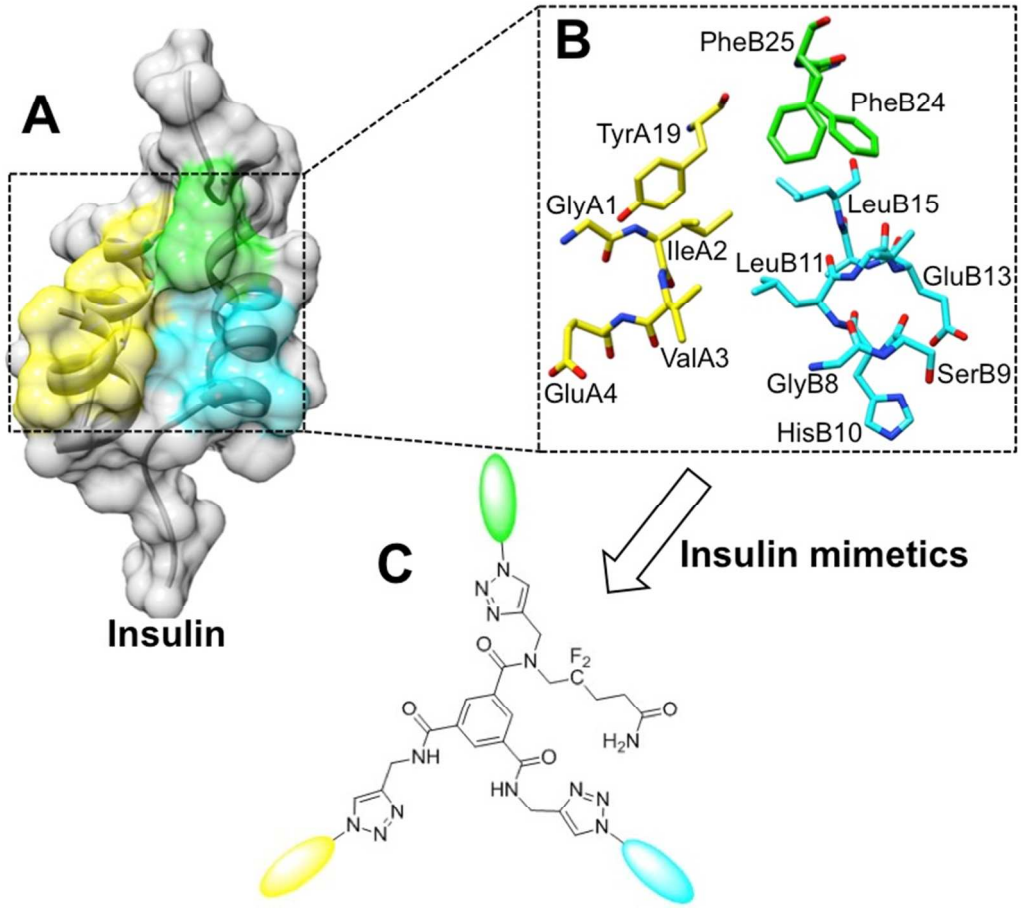

Figure 2. The proposed strategy for the development of insulin mimetics. (A) The molecular surface of the active (i.e., receptor-bound) conformation of insulin is represented here by the crystal structure of AsnB26-insulin, pdb code 4ung, from Ref.[24] Examples of IR-binding amino acids (epitopes) are depicted in yellow (GlyA1, IleA2, ValA3, GluA4 and TyrA19), green (PheB24 and PheB25) and blue (GlyB8, SerB9, HisB10, LeuB11, GluB13 and LeuB15). Only a subset of IR-binding amino acids is shown here and all IR-binding amino acids of insulin are listed in the main text. (B) The selected IR-binding epitopes were extracted from the structure of AsnB26-insulin and should be mimicked by the compounds derived from scaffold **I**, as shown in (C).

RESULTS

Design of the Libraries. Scaffold **I** was synthesized using the procedure described in our previous work[(10)] and employing several improvements (see the Supplementary Information).

The 30 azides used for the derivatization of scaffold **I** are shown in Table 1, and their syntheses are described in the Supplementary Information. The synthesis of specific azides was

generally motivated by mimicking the character of IR-binding amino acids in insulin (i.e. lipophilic, aromatic, acidic or polar, see above).

We used a split-and-mix strategy, which allows the simple generation of defined mixtures of the compounds.[35-37] For the coupling to the individual arms (**A**, **B** or **C** in Table 1) of scaffold **I**, we divided the azides into three sets (**A**-**C**). Each set is composed of 10 azides with varying physicochemical properties (aromaticity, charge, and lipophilicity) to achieve a greater chemical diversity in the final compounds. Each of the azides is present in only one set (the azides from set **A** were only inserted at position **A** of the scaffold, and so on).

Table 1. **Sets of Azides (A-C) Used for the CuAACs on the Individual Arms (A-C, Respectively) of Scaffold I.**

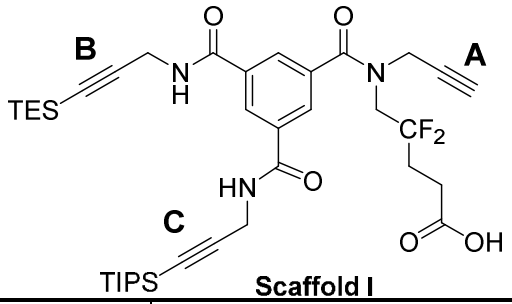

Scaffold I

Azide set	**A**	**B**	**C**
1	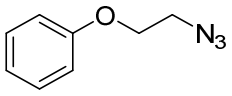	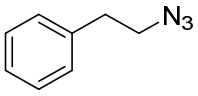	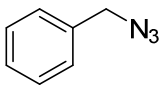
2	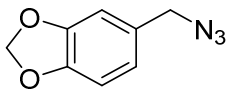	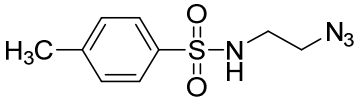	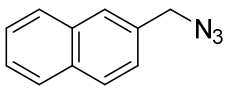
3	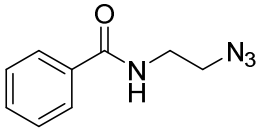	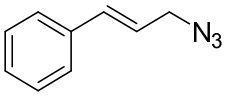	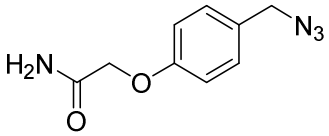
4	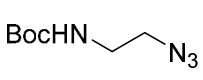	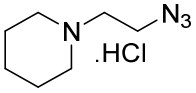	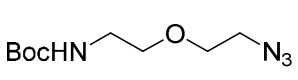

5	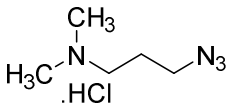		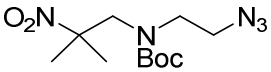
6	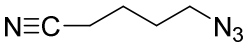	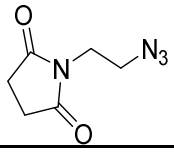	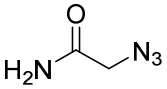
7	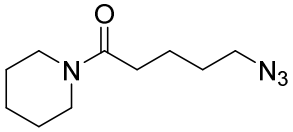	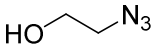	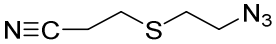
8	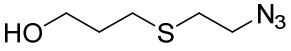	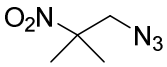	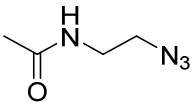
9	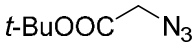	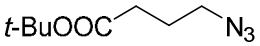	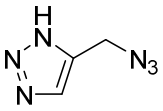
10	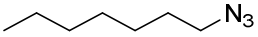	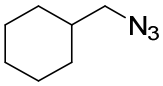	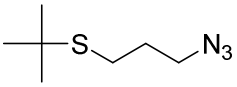

Synthesis and Deconvolution of the Library. For the solid-phase synthesis of the library, we used the PEG-based ChemMatrix resin[38,39] because it gave satisfactory results for CuAACs with the $CuSO_4$/sodium ascorbate system in tBuOH/H_2O.[10,40] We used the Ramage linker, which can be cleaved by low concentrations of TFA (3-5%) to generate the terminal amides.[41]

The synthesis of the library is shown in Scheme 1. We prepared ten sub-libraries, labeled **C1** to **C10**, to reflect the presence of a single and specific azide from set **C** in each of the sub-libraries. Each sub-library contained 100 compounds, which arose from the combinations between the azides from sets **A** and **B**. Thus, the total library was composed of 1,000 compounds, and each of these compounds had three different azides on arms **A**-**C**. The chemistry, which was described in detail in our previous report,[10] was easy to implement; dry or inert conditions are not required, all reactions are performed at room temperature and the synthesis of the library is completed within 14 days.

After cleavage from the resin and subsequent Boc/tBu deprotection with trifluoroacetic acid (TFA, steps f and g in Scheme 1), the ten mixtures were extracted with diethyl ether to remove the non-polar impurities (particularly the triisopropylsilane (TIS) derivatives; TIS was used to scavenge the possible carbocations).

We supposed that some residual copper may be present in the mixtures obtained after the diethyl ether extraction and performed an ICP analysis of the sub-libraries **C9** and **C10** (these two sub-libraries appeared particularly bluish). The analyses showed a copper content of approximately 1% (w/w). We subsequently investigated different purification methods to remove copper: separation on C-4 or C-8 SPE cartridges, treatment with a thiol-based cation exchange resin, fast purification by preparative RP-HPLC or treatment with gaseous hydrogen sulfide (H_2S) (for details see the SI). The treatment of the sub-libraries with hydrogen sulfide, followed by filtration, was the most optimal, simple, short and efficient method. Briefly, the sub-libraries were dissolved in ACN/H_2O, and gaseous hydrogen sulfide was blown at the surface of these solutions upon stirring. After precipitation of the copper sulfides (apparition of a dark-brown precipitate), the solutions were filtered and lyophilized. Elemental analyses showed that the amount of copper in sub-libraries **C9** and **C10** dropped from 1% to 0.06% and 0.01% (w/w), respectively.

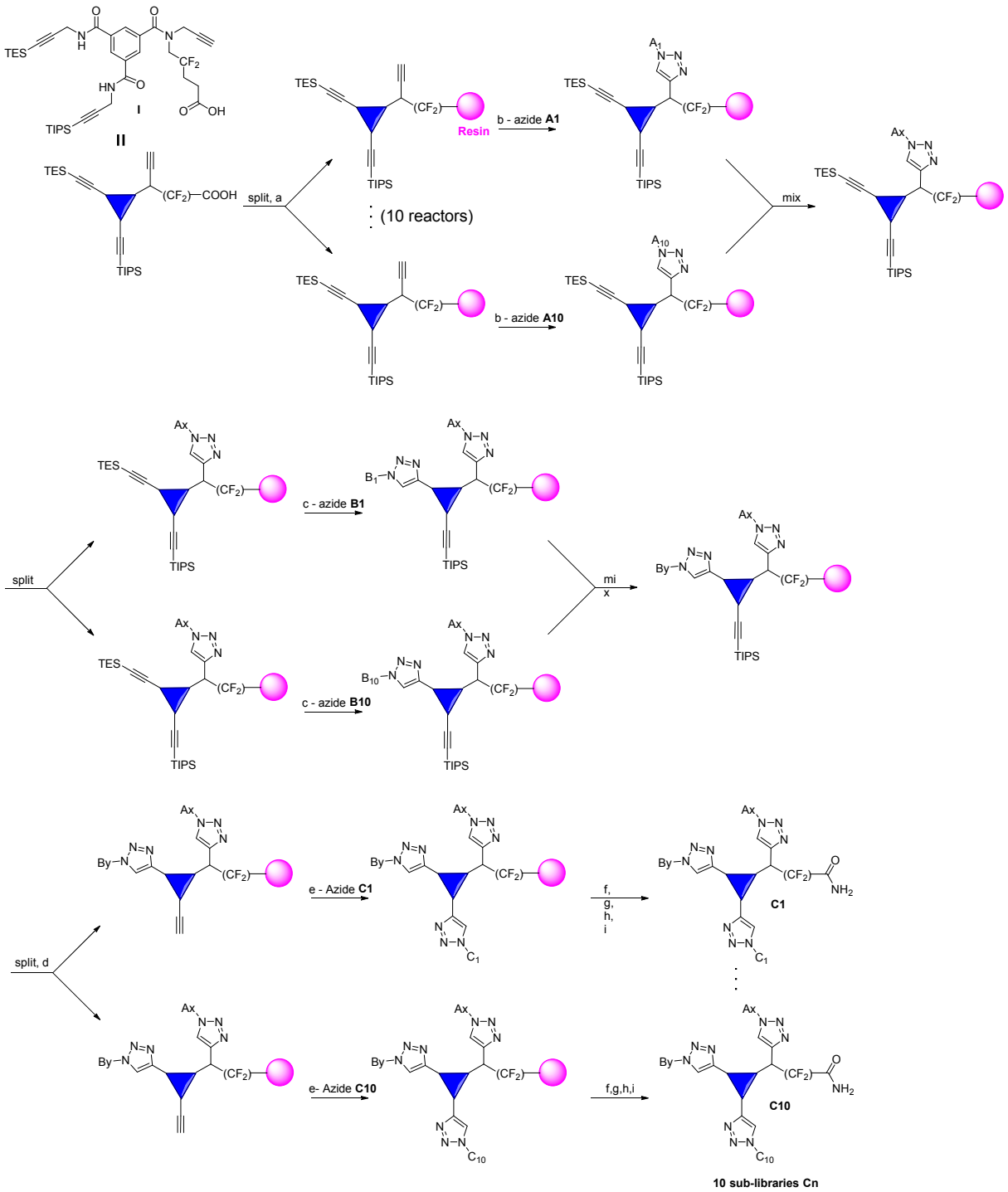

Scheme 1. Synthesis of the sub-libraries **C1** to **C10**. Reagents and conditions: (a) Ramage ChemMatrix® (2 equivalents, 200 µmol/reactor), PyBroP (2 equivalents), DIPEA (4 equivalents), DMF, 16 h; (b) azide **A** (5 equivalents), sodium ascorbate (0.5 equivalent), $CuSO_4.5H_2O$ (0.1 equivalent), *t*BuOH/H_2O, 2×16 h; (c) azide **B** (5 equivalents), sodium ascorbate (10 equivalents), $CuSO_4.5H_2O$ (5 equivalents), *t*BuOH/H_2O, 16+5 h; (d) TBAF (5

equivalents), DMF, 3×1.5 h; (e) azide **C** (5 equivalents), sodium ascorbate (0.5 equivalent), $CuSO_4.5H_2O$ (0.1 equivalent), *t*BuOH/H_2O, 2×16 h; (f) 5% TFA in DCM, 2×30 minutes; (g) 50 % TFA in DCM + 2% TIS, 2 h; (h) Diethyl ether extraction (20 mL); (i) treatment with gaseous H_2S in ACN/H_2O (30 minutes) followed by filtration.

Next, based on the biological results (see below), we deconvoluted sub-library **C4**, as shown in Scheme 2. We repeated the synthesis described in Scheme 1, but omitted the second split-and-mix process and only introduced the azide **C4** during the third CuAAC. Consequently, we obtained ten sub-libraries, **C4B1-C4B10**, which contained 10 compounds each that only varied at position **A**. As some sub-libraries maintained a dark-brown coloration after treatment with hydrogen sulfide and filtration, we performed the ICP analyses of sub-libraries **C4B3** and **C4B7** (these sub-libraries had a particularly dark color). The copper content in these mixtures was 0.17% and 0.34% (w/w), respectively, and was higher than sub-libraries **C9** and **C10**.

Because the biological activity observed in **C4** was not detected in sub-libraries **C4B1-C4B10** (see below), we considered physical-chemical arguments, selected sub-library **C4B7** (which contains compounds that had the lowest molecular weights and displayed good solubility in water) to be deconvoluted and thus synthesized compounds **C4B7A1-C4B7A10** (Scheme 2). Figure S1 shows the superimposed RP-HPLC profiles of sub-library **C4B7** and compounds **C4B7A1-C4B7A10**, which could be easily identified in sub-library **C4B7**. LC-MS analysis of sub-library **C4B7** also confirmed the presence of the expected compounds **C4B7A1-C4B7A10** (Figure S2). The crude compounds **C4B7A1-C4B7A10** were prepared with satisfactory HPLC purities ranging from 46 % to 71% (see Table S1).

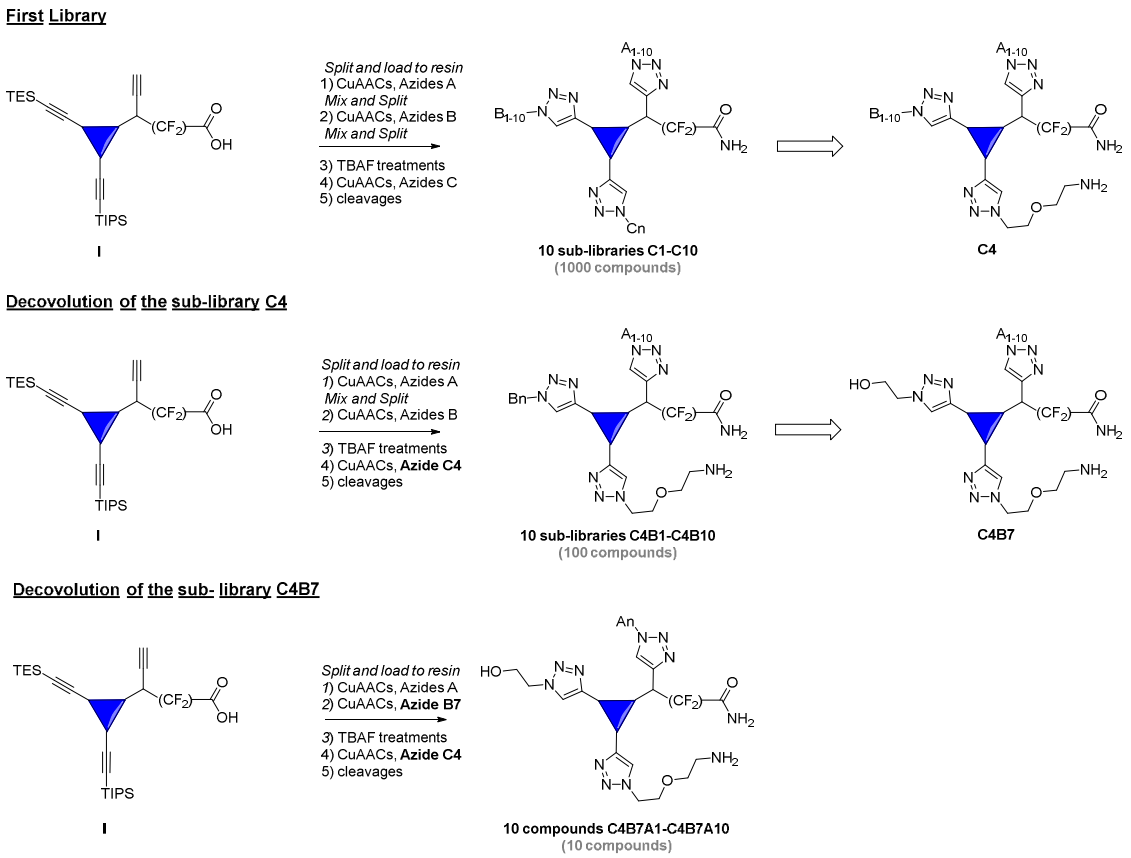

Scheme 2. Overview of the synthesis of sub-libraries **C1-C10** and **C4B1-C4B10** and compounds **C4B7A1-C4B7A10**. The conditions are the same as the conditions described in Scheme 1.

Biological Evaluations of Sub-Libraries C1-C10, C4B1-C4B10 and Compounds C4B7A1-C4B7A10. First, based on the concentrations determined by ^{19}F NMR, we prepared 1 mM stock solutions of individual libraries in 100 mM Hepes/NaOH buffer, pH 7.5 (see Experimental Methods). The concept and the methodology of the determination of the concentration of scaffold **I**-derived compounds were described in detail in our previous papers.[10,40]

All libraries and compounds were tested for binding to both IR-A and the IGF-1 receptor (IGF-1R). The resulting concentrations of the compounds in all experiments were 0.1 mM, unless stated otherwise. Further, the ability of the libraries and compounds to stimulate the autophosphorylation of both receptors was assessed. There were no significant differences between the abilities of the two types of receptors (IR-A and IGF-1R) to bind to the compounds

or in the abilities of the compounds to stimulate the receptors. For this reason, we only show the data obtained for IR-A.

The results of the binding of sub-libraries **C1**-**C10** to IR-A are shown in Supplementary Figure S3. Briefly, at a 0.1 mM concentration, none of the sub-libraries effectively inhibited the binding of ^{125}I-insulin to IR-A. However, two sub-libraries, **C4** and **C2**, showed a weak but significant ability to induce IR-A autophosphorylation (Figure 3).

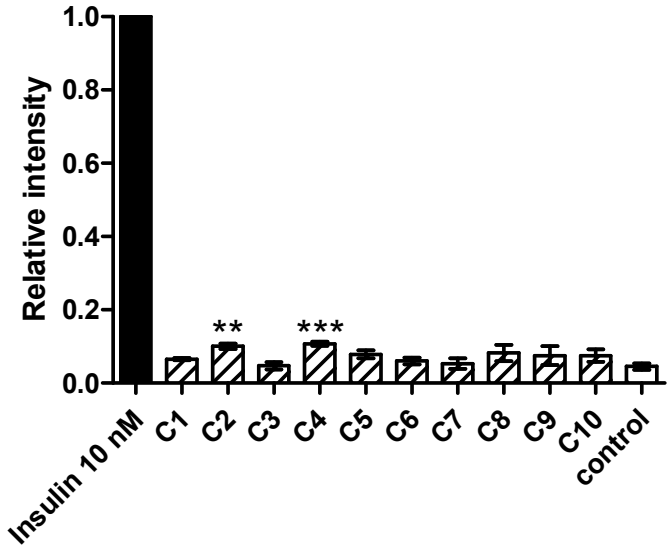

Figure 3. Stimulation of IR-A phosphorylation by 0.1 mM concentrations of sub-libraries **C1-C10.** The experimental values were related to the activity of 10 nM human insulin. Asterisks indicate that the autophosphorylation of the receptor induced by the library differs significantly (** $p < 0.01$, *** $p < 0.001$) from the control (background).

In the next step, we tested the biological activities of sub-libraries **C4B1**-**C4B10**, each of which contain 10 compounds (Scheme 2). None of these sub-libraries significantly inhibited the binding of ^{125}I-insulin to IR-A (Figure S4) or induced IR-A autophosphorylation (Figure S5) at 0.1 mM. Finally, the same absence of biological activity was observed for compounds **C4B7A1**-**C4B7A10**, which do not bind to IR-A (Figure S6) or activate IR-A (Figure S7).

Searching for Active Compounds in Sub-Library C4. We wanted to understand why the weak but significant biological activity of sub-library **C4** was not observed in sub-libraries **C4B1-C4B10.** Therefore, we verified whether some active compound(s) could be isolated from

sub-library **C4**. After several iterative purifications by RP-HPLC, we found two fractions (**C4-1** and **C4-2**) that were able to activate IR-A (Figure 4A and 4B). These fractions were analyzed by high-resolution mass spectrometry (HRMS), and the experimental HRMS signals were attributed to compounds **C4B2A10** and **C4B3A6** (Figure 4A).

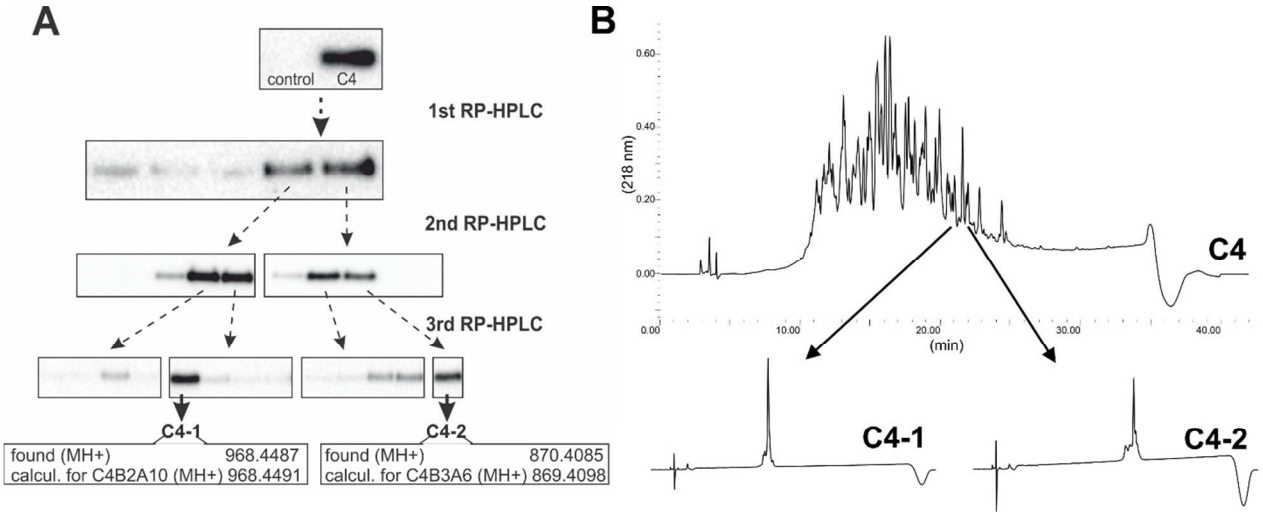

Figure 4. Simplified scheme for the separation of sub-library **C4** by preparative RP-HPLC. (A) Stimulation of IR-A phosphorylation by the fractions isolated from sub-library **C4** using preparative RP-HPLC. Four to five fractions were collected during each successive chromatography step and tested for their ability to stimulate the cells. Phosphorylated receptors were detected on western blots using an anti-phospho-IGF-1R β-subunit (Tyr1131) / IR β-subunit (Tyr1146) antibody. The cells were stimulated with 0.1 mg/mL fractions for 10 min. Fractions **C4-1** and **C4-2** were analyzed by HRMS and the major m/z signals detected were attributed to compounds **C4B2A10** and **C4B3A6**. (B) RP-HPLC chromatograms of the crude sub-library **C4** and the two biologically active isolated fractions (**C4-1** and **C4-2**).

Synthesis of the Focused Library. These results encouraged us to synthesize compounds **C4B2A10** and **C4B3A6** and to design a small focused library of compounds that were derivatized with the azides (**A6**, **A10**, **B2** and **B3**) found in compounds **C4B2A10** and **C4B3A6**. We decided to preserve azide **C4** at position **C** of the scaffold. Varying the two remaining positions with four different azides would yield 16 different compounds (4^2). However, we only prepared 10 compounds (including **C4B2A10** and **C4B3A6**) to reduce the number of syntheses,

and the structures are shown in Table 2. The six remaining compounds (**C4A10B2**, **C4A6B3**, **C4A10BA6**, **C4A10B3**, **C4A6B2** and **C4B2B3**) were not prepared because they differ from the compounds shown in Table 2 only in the swapping of azides at positions A and B. The compounds shown in Table 2 were purified by RP-HPLC and obtained in satisfactory yields, ranging from 22% to 64% (Table S1). The chromatograms of the crude compounds are shown in supplementary Figures S8 and S9, and their purities ranged from 51-74% (Table S1).

Table 2. **Structures of the Compounds from the Focused Library.**

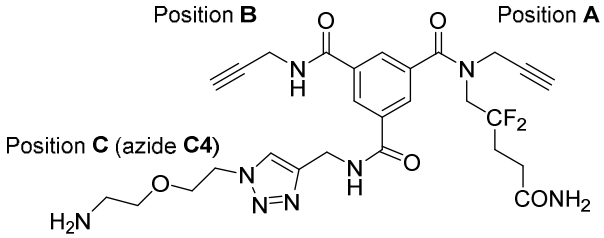

Azide at position **C**	Azide at position **B**	Azide at position **A**	Code of the compound
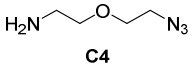 C4	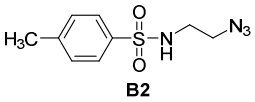 B2	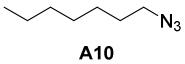 A10	**C4B2A10**
	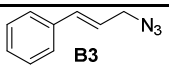 B3	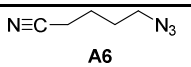 A6	**C4B3A6**
	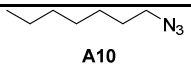 A10	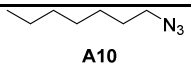 A10	**C4A10A10**
	 A6	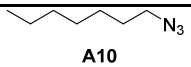 A10	**C4A6A10**
	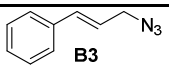 B3	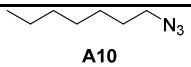 A10	**C4B3A10**
	 A6	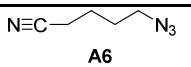 A6	**C4A6A6**
	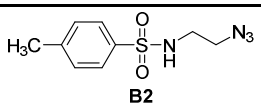 B2	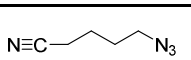 A6	**C4B2A6**
	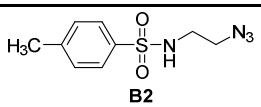 B2	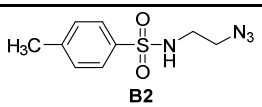 B2	**C4B2B2**

			C4B3B2
			C4B3B3

The compounds were then tested for their ability to induce IR-A autophosphorylation. However, none of the new compounds showed significantly stronger biological activity than did the "original" **C4** sub-library or fractions **C4-1** and **C4-2**, and only compounds **C4B2A10** and **C4B3A6** weakly activated IR-A at a concentration of 0.1 mM (Figure 5A). Finally, we checked whether the purified compound **C4B2A10** can compete with ^{125}I-insulin in binding to IR-A. We found that this compound weakly inhibits the binding of insulin to IR-A at a concentration of 0.1 mM (Figure 5B).

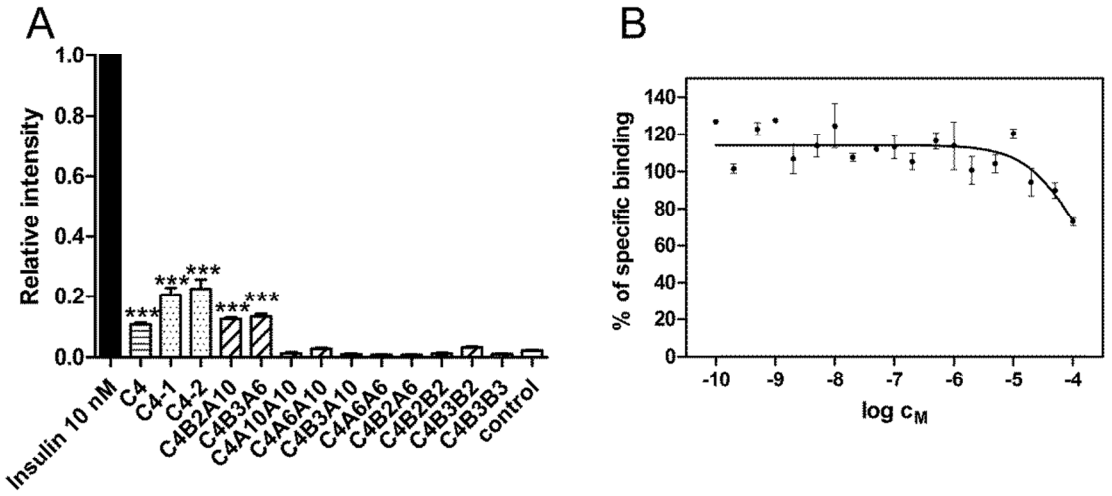

Figure 5. (A) Stimulation of IR-A authophosphorylation by compounds from the focused sub-library at a concentration of 0.1 mM compared with the original **C4** library and fractions **C4-1** and **C4-2** isolated from the **C4** library. The experimental values are related to the activity of 10 nM human insulin. The control is the buffer in which the compounds were solubilized. (B) Inhibition of the binding of ^{125}I-insulin to IR-A by compound **C4B2A10**.

DISCUSSION

Synthesis. An important aspect of combinatorial synthesis is to establish a convenient synthetic protocol that affords the desired compounds (often present in mixtures) with purities

and yields that are sufficient for reliable biological evaluation. The data shown in the Supporting Information (e.g., Figures S1, S2, S8, and S9 and Table S1) show the suitability of the synthetic protocol for generating large sets and mixtures of diverse compounds.

Another important condition for combinatorial synthesis is the versatility and robustness of the synthetic method; i.e., the applied chemistry should not interfere with the different functionalities present in the precursor compounds. Here, we reported the successful syntheses of compounds with primary alcohol (azide **B7**), ether, carbamate (azide **C4**), vinylbenzene (azide **B3**), catechol (azide **A2**), nitrile (azide **A6**), tertiary amine (azide **A5**), thioether amide (azide **A8**) or sulfonamide (azide **B2**) moieties and obtained the desired compounds without side-reactions. The main impurities observed on LC-MS (not shown) resulted from the double azide addition (both at the free and the TES-protected alkyne) during the first CuAAC (e.g. the compound **C4A3A3** was also isolated together with **C4B7A3**). This is not surprising, as the TES group could be cleaved under the conditions used for the CuAAC. Overall, these results confirm the suitability of the method for combinatorial applications. However, we should also mention two possible limitations of our methodology: the final TFA cleavage that precludes acid-labile functions, and the treatment with hydrogen sulfide is not suitable for disulfides.

The strategy of orthogonal TIPS/TES protection of terminal alkynes was first developed in Aucagne's group,[(42)] who selectively deprotected the TES group by using Ag(I) salts and these conditions were recently applied by Liskamp's group.[43,44] However, under our experimental conditions, silver deposits appeared on the resin, which disabled further synthesis. We solved this problem by performing the CuAAC directly on the TES-protected terminal alkyne and by using an excess of copper(II) and sodium ascorbate.[10,40] Under these conditions, the TES group is selectively deprotected and the cycloaddition with the azide occurs in one-pot. The mechanism of the TES cleavage during high copper load CuAAC is unclear and is currently being investigated in our laboratory. Consequently, the only difficult point during the synthesis was removing the copper that accumulated in the resin, particularly during the one-pot TES-deprotection/CuAAC that was performed with excess copper, which could hypothetically interfere with the bioassays. It was not trivial to remove the copper because we needed to establish a general method that was suitable for all of the compounds in our library, which have different functionalities, polarities and charges. After investigating various alternative methods (see the Supporting Information), we opted to treat the crude mixtures/compounds in solution with hydrogen sulfide after cleavage

from the resin; this strategy led to the precipitation of copper that could be filtered from the solution. This method allowed us to reduce the copper content in sub-libraries **C1**-**C10** to a negligible level. However, the copper content in sub-libraries **C4B1**-**C4B10** and in compounds **C4B7A1**-**C4B7A10** remained higher, despite the application of the same treatment (Table S1). These variations can be explained by the particular functionality of some compounds; for instance, the carboxylic acid moiety of **C4B7A9** (copper content of approximately 7% w/w) may interfere with the precipitation of copper sulfide. Thus, we experimentally verified that the presence of copper sulfide in concentrations up to 300 μM did not positively or negatively interfere with our cellular binding assays to avoid any ambiguity in interpreting the biological assays (data not shown). We have not found other data in the literature on the copper contents after solid-phase CuAAC (recently reviewed in Castro et al. in Ref.[45]) that we could compare with our data. We are now also exploring alternative methods for TES deprotection.

Biological Activity. Only sub-libraries **C4** and **C2** significantly activated IR-A at 0.1 mM. However, the degree of receptor autophosphorylation by **C4** and **C2** was much lower than the activation induced by 10 nM human insulin (Figure 3); moreover, it was not convincingly (possibly with the exception of weak inhibition by **C4**) accompanied by the inhibition of insulin binding (Figure S3). This result could indicate that the compounds bind to another site on the receptor than the insulin binding site or that the binding assay is less sensitive than our receptor autophosphorylation assay. However, the identification of any IR activators would also be interesting for further development of insulin agonists. Therefore, we selected sub-library **C4** and prepared sub-libraries **C4B1**-**C1B10**, but none of these mixtures activated IR-A or inhibited insulin binding (Figures S4 and S5).

Sub-library **C4** contains 100 different compounds, and it can be expected that the weak biological activity of **C4** could originate either from a sum of the activities of several (or many) weaker compounds or from the activity of a single active compound, which would be present in the tested **C4** mixture at a concentration of 0.001 mM. The presence of only a single active compound should be revealed by the stronger bioactivity (compared to **C4**) of one of the **C4B1**-**C4B10** sub-libraries. However, this stronger bioactivity was not observed, indicating that the bioactivity of **C4** is instead composed of the contributions from several weak compounds. We attempted to isolate active compound(s) from **C4** by preparative HPLC to verify this hypothesis. This iterative process yielded two active fractions, **C4-1** and **C4-2** (Figure 4), in which we

detected m/z signals for compounds **C4B2A10** and **C4B3A6**. Based on this finding, we prepared these two compounds and a small "focused" library of 8 compounds (Table 2), where we maintained the **C4** azide and varied the **B2**, **B3**, **A6** and **A10** azides (to verify whether some combinations of these "active" azides could result in more potent compounds). We should note that the original library contained only compounds with three different azides, whereas the focused library contained compounds with the same azide at two different positions. The testing of this "focused" library showed that only compounds **C4B2A10** and **C4B3A6** that were identified by MS were able to activate IR-A, but their activities were weaker than the original **C4-1** and **C4-2** fractions (Figure 5A). This result could mean that these fractions are not pure and still contain some other active compounds, which is indeed probable (see Figure 4). Moreover, we found that compound **C4B2A10** is able to displace insulin from its IR-A receptor (Figure 5B), albeit only weakly and at a concentration of 0.1 mM, which could indicate that the compound at least partially binds to the insulin binding site on IR. We can only speculate why the activities of compounds **C4B2A10** and **C4B3A6** were not manifested as significant activities in the **C4B2** and **C4B3** mixtures. The reason may be the weak activities of **C4B2A10** and **C4B3A6**, which are only "visible" at 0.1 mM; if these compounds displayed some activity in the **C4B2** and **C4B3** mixtures (also tested at 0.1 mM), their concentration would be 0.01 mM and would be too low to elicit IR-A phosphorylation and detect binding. This finding rather supports our hypothesis (see above) that the apparent biological activity of the **C4** mixture (containing 100 compounds) could be due to a simultaneous additive effect of several or many compounds with weak activities (including **C4B2A10** and **C4B3A6** representing probably more active compounds among them). However, it is possible that some other phenomenon is behind the loss of activity. For example, we cannot exclude the presence of some more active by-product in **C4** (non-identified), which we omitted during purification and which was not present in **C4B1**-**C4B7**.

In summary, this is our first attempt to develop non-peptide insulin mimetics. We designed a combinatorial library of tri-functional compounds that were derivatized with 30 different azides, which should mimic the IR-binding epitopes in insulin and bind to and activate IR. Despite the unsatisfactory biological results, this study represents a unique example of targeting IR with a set of non-peptide compounds that were specifically designed and synthesized for this purpose. Other published attempts at identifying insulin mimetics were based on molecular modeling and/or screening of virtual or in-house libraries of compounds,[26-30] phage display peptide

libraries[31-33] or oligonucleotide aptamers.[34] The reason for the lack of significant biological activity of our library of 1,000 compounds derived from scaffold **I** may be the selection of inappropriate azides, the low diversity of the library or the "incompatibility" of the scaffold **I** structure with the IR receptor. However, considering the high sensitivity of insulin receptor to modifications of insulin structure, this result is not completely surprising and confirms the great difficulty of the task. Insulin is a 51 amino acid hormone, and the deletion of only eight C-terminal amino acids of the B-chain leads to an approximately 2,500-fold decrease in the binding affinity from 0.2 nM to 500 nM (non-published data from our laboratory). Moreover, some structural modifications in the B-chain, C-terminal segment of insulin[20] or even some single amino acid modifications in insulin, e.g., at position B24 (Ref.[17]), B8 (Ref.[19]) or A2 (Ref.[46]) have similar disruptive effects on insulin binding activity. However, we still believe that the idea of non-peptide activators of the insulin receptor is realistic and we are encouraged by the result reported by Schlein et al.[27], who identified the small molecule thymolphtalein (MW 430) as an agonist that displaced insulin from IR (K_d approximately 10^{-6} M). Moreover, we believe that the selection of more convenient ligands (e.g., peptides or peptidomimetics) for modifying scaffold **I** and/or a larger sized library could lead to more valuable biological results. Nevertheless, despite the negative biological results, this work has enabled us to test our synthetic methodology and to prove its robustness and reliability for the synthesis of combinatorial libraries on the solid phase using our home-made library of azides with varying functionalities.

EXPERIMENTAL METHODS

Chemistry

General Information. Unless stated otherwise, the reagents and solvents used in this study were obtained from commercial suppliers and used without purification. The solvents were evaporated at 55 °C and 2 kPa, and the products were dried over sodium hydroxide at r. t. and 100 Pa. Analytical RP-HPLC chromatography of the compounds was performed on a Waters HPLC system (Waters 1525 Binary HPLC Pump and Waters 2787 Dual λ Absorbance Detector) using a Nucleosil 120-5 C8 column (250 x 4.6 mm, 5 μm, Macherey-Nagel) at a flow rate of 1 mL/min. The compounds were detected at 218 and 254 nm. Preparative RP-HPLC chromatography of the compounds was conducted on the same Waters HPLC system using a Vydac 214TP101522 C4 column (250 × 22 mm, 10–15 μm, Columbia, MD, USA) at a flow rate

of 9 mL/min. The detection was the same as for the analytical HPLC. MS spectra were obtained on an LTQ-Orbitrap XL FTMS mass spectrometer (Thermo Fisher, Bremen, Germany) in electrospray ionization mode (Waters) or, in the case of HRMS (EI), on a GCT Premier (Waters). ^{19}F NMR spectra were measured on a Bruker AVANCE-500 instrument at 470.4 MHz. For the quantitative analyses, the ^{19}F proton decoupled spectra were measured with suppression of heteronuclear NOE during a relaxation delay (3 s). A known amount of $BrCF_2COOEt$ was added to the measured solution and used as an internal standard. The copper contents were determined by ICP with a Spectro Arcos ICP-OES analyzer (plasma power: 1450 W; coolant flow Ar: 1.0 L/min; auxiliary flow: 0.8 L/min; nebulizer flow: 0.75 L/min; sample introduction system: Mod Lichte; cyclonic spray chamber; matrix: 4% HNO_3 (w/w); and internal standard Y (2 mg/kg)).

The syntheses of the 30 azides (shown in Table 1) used for the derivatization of scaffold **I** are described in detail in the Supplementary Information.

Combinatorial Syntheses on the Solid Phase. *Loading onto the resin:* Ten fritted polypropylene syringes (20 mL) were loaded with Ramage ChemMatrix® resin (385 mg each, 200 μmol, 0.52 mmol/g, Aldrich lot BCBN4288V) with free amino groups. The resins were swelled in MeOH, DCM, and DMF (10 minutes each) using 10 mL of solvent/g of resin. The resins were then washed with 3×5 mL of DMF (1 min each). The following freshly made solutions were added to each resin: a 0.1 M solution of scaffold **I** in DMF (1 mL, 100 μmol), a 0.2 M solution of PyBROP in DMF (1 mL, 200 μmol), and a 0.4 M solution of DIPEA in DMF (1 mL, 400 μmol). The 10 syringes were stirred (at 360° vertically) at room temperature for 16 h. The resins were finally washed with 3×5 mL of DMF, MeOH, DCM, and DMF (1 min each).

First CuAAC: The resins in the ten syringes were washed with 3×5 mL of MeOH and *t*BuOH/water (1:1, v/v) (1 min each). The following freshly made solutions were sequentially added to the resins: i) a 0.5 M solution of azide A in *t*BuOH/water (1:1, v/v) (1 mL, 500 μmol), ii) a 0.05 M solution of sodium ascorbate in *t*BuOH/water (1:1, v/v) (1 mL, 50 μmol), and iii) a 0.01 M solution of copper(II) sulfate pentahydrate in *t*BuOH/water (1:1, v/v) (1 mL, 10 μmol). Two couplings were performed, each for 16 h at room temperature. Between couplings, the resins were washed with 3×5 mL of *t*BuOH/water (1:1, v/v) (1 min each). The resins were finally washed with 3x5 mL of *t*BuOH/water (1:1, v/v), DMF, H_2O, MeOH, DCM, and DMF (1 min each).

Note: Aqueous solutions of sodium ascorbate (0.5 M) and copper(II) sulfate pentahydrate (0.1 M) were first prepared and then diluted in *t*BuOH/water to prepare the sodium ascorbate and copper(II) sulfate pentahydrate solutions in *t*BuOH/water (1:1, v/v).

Split and mix procedure: The resins were transferred into a 1 L beaker with DMF. The resin was suspended in DMF and gently shaken on a moving plate for 30 minutes. The resin was transferred into a tarred fritted Buchner funnel and the DMF was removed by suction. The resin was then split into ten equal portions and transferred to ten fritted polypropylene syringes.

One-pot TES deprotection and second CuAAC: The resins were washed with 3×5 mL of MeOH and *t*BuOH/water (1:1, v/v) (1 min each). The following freshly made solutions were sequentially added to the resins: i) a 0.25 M solution of azide B in *t*BuOH/water (1:1, v/v) (2 mL, 500 μmol), ii) a 0.5 M solution of sodium ascorbate in *t*BuOH/water (1:1, v/v) (2 mL, 1000 μmol), and iii) a 0.25 M solution of copper(II) sulfate pentahydrate in *t*BuOH/water (1:1, v/v) (2 mL, 500 μmol). Two couplings were performed for 16 h and 5 h at room temperature. Between couplings, the resins were washed with 3×5 mL of *t*BuOH/water (1:1, v/v), AcOH (to help removing copper salts), H_2O, DMF, DCM, MeOH and *t*BuOH/H_2O (1:1, v/v) (1 min each). The resins were finally washed with 3x5 mL of *t*BuOH/water (1:1, v/v), AcOH, H_2O, MeOH, DCM and DMF (1 min each).

Note: It is necessary to first prepare the aqueous solutions to dissolve the sodium ascorbate and copper(II) sulfate pentahydrate in *t*BuOH/water (1:1, v/v). Hence, we first prepared aqueous solutions of sodium ascorbate (1 M) and copper(II) sulfate pentahydrate (0.5 M), which were then diluted with *t*BuOH.

TIPS deprotection: The resins were washed with 3×5 mL of DMF (1 min each). A solution of TBAF (500 μL of a 1 M solution in DMF, 500 μmol) in DMF (3 mL) was added to each reaction. Three treatments were performed, each for 1.5 h at room temperature. Between each treatment, the resins were washed with 3×5 mL of DMF (1 min each). The resins were finally washed with 3×5 mL of DMF, H_2O, AcOH, H_2O, MeOH, DCM and DMF (1 min each).

Third CuAAC: The resins were washed with 3×5 mL of MeOH and *t*BuOH/water (1:1, v/v) (1 min each). The following freshly made solutions were sequentially added to the resins: i) a 0.5 M solution of azide C in *t*BuOH/water (1:1, v/v) (1 mL, 500 μmol), ii) a 0.05 M solution of sodium ascorbate in *t*BuOH/water (1:1, v/v) (1 mL, 50 μmol), and iii) a 0.01 M solution of copper(II) sulfate pentahydrate in *t*BuOH/water (1:1, v/v) (1 mL, 10 μmol). Two couplings were

performed, each for 16 h at room temperature. Between the two couplings, the resins were washed with 3×5 mL of *t*BuOH/water (1:1, v/v) (1 min each). The resins were finally washed with 3x5 mL of *t*BuOH /water (1:1, v/v), DMF, H_2O, DMF, DCM, MeOH and DCM (1 min each).

Cleavage from the resin: The resins were transferred to fritted reactors with DCM and dried over NaOH in desiccators for 1 h. Each resin was then treated with a 5% TFA/DCM solution (10-15 mL) for 30 minutes. The resins were washed with 3×5 mL of 5% TFA/DCM (1 min each). The resulting solutions (filtrates) were transferred to tarred 100 mL flasks and evaporated. The resins were treated a second time with a 5% TFA/DCM solution (10-15 mL, 30 minutes) and washed with 3×5 mL of 5% TFA/DCM and AcOH (1 min each). All cleavage and washing solutions (filtrates) for a given compound were transferred to the corresponding 100 ml flask and evaporated to dryness. The yields (in mg) obtained for each sub-library or single compound are shown in Table S2.

Boc/tBu deprotection: A 50 % TFA/DCM solution with 2% TIS (5 mL in total) was added to the 100 mL flasks containing the sub-libraries or single compounds. The resulting mixtures were stirred at room temperature for 2 h and evaporated to dryness.

Diethyl ether extraction: Diethyl ether (20 mL) was added to each 100 mL flask. The resulting suspensions were sonicated for 5 minutes. The solutions were transferred to 50 mL falcons and centrifuged (5 minutes, 7,200 rpm, 20 °C). The supernatants were discarded and the remaining solids were transferred back to the corresponding 100 mL flask using ACN/H_2O solutions and lyophilized. We wished to verify that no desired product was extracted into the diethyl ether during the extraction. We chose sublibrary **C2** because it is the most lipophilic sub-library. Therefore, we performed HPLC analyses of sub-library **C2** before and after diethyl ether extraction, as well as an MS analysis of the diethyl ether extract. These analyses revealed that no major loss of the compounds occurred during the diethyl ether extraction (Figures S10 and S11).

Treatment with gaseous hydrogen sulfide: After the diethyl ether extraction, the sub-libraries were dissolved in 30-50% ACN/H_2O (3 mL). Gaseous hydrogen sulfide (H_2S) was blown at the surface of the solutions while stirring. The solutions were allowed to stand for 30 minutes and slowly turned from light brown to black, which reflected the formation of the copper sulfide precipitate. The mixtures were then filtered through a Rotilabo® PVDF filter (0.22 µm), lyophilized and weighed. The yields (in mg) are presented in Table S3. Sublibrary **C1** (20.8 mg)

was dissolved in 40% ACN/H_2O (3 mL) and the solution was analyzed by HPLC to verify that no compounds were lost during this process. Then, the solution was treated with hydrogen sulfide, as described above. After filtration, the filtrate was again analyzed by HPLC and we verified that the two HPLC chromatograms were identical (Figure S12).

CAUTION: Hydrogen sulfide is a toxic gas that must only be manipulated in the fume hood.

Quantification by ^{19}F NMR. The final sub-libraries were stored as frozen solutions in 40% ACN/H_2O at -80°C. For biological testing, a precise volume of each of these solutions was transferred to an Eppendorf tube and lyophilized. The dry samples were transferred to NMR tubes using d_6DMSO (3×0.15 mL). A solution of commercial ethyl bromodifluoroacetate (100 µL of a 0.1 M solution in d_6DMSO) was added to the NMR tube as an internal standard.[10] Integration over the region corresponding to the CF_2 signals and comparison to the standard CF_2 signal allowed us to quantify the compounds containing the scaffold. Consequently, the concentrations of the stock solutions in the scaffold-derived compounds could be calculated. As discussed above, the main impurities found in the single compounds are due to double incorporation during the first CuAAC (the same azide clicked into the arms A and B). Although we were not able to characterize such impurities in the library mixtures, they should be present. As such impurities contain the CF_2-labelled arm, the concentrations of the libraries in desired compounds is probably slightly over evaluated.

Synthesis of the focused library. Compounds **C4B2A10**, **C4B3A6**, **C4A10A10**, **C4A6A10**, **C4B3A10**, **C4A6A6**, **C4B2A6**, **C4B2B2**, **C4B3B2** and **C4B3B3** were synthesized on the solid phase as described above (section 1.2), starting with 100 µmol of scaffold **I**. The RP-HPLC chromatograms of the crude compounds are shown in the Supporting Information (Figures S8 and S9). The crude compounds were then purified by preparative RP-HPLC and the yields over the whole process were calculated (Table S1). The purities of the HPLC-purified compounds were above 95 % in all cases.

Analyses of the libraries. Given the complexity of sub-libraries **C1-C10**, these sub-libraries were not analyzed by MS or LC-MS. However, sub-library **C4B7** was analyzed by LC-MS (Figure S2), confirming the presence of the expected 10 compounds, **C4B7A1-C4B7A10**. Compounds **C4B7A1-C4B7A10** and the compounds from the focused library (see Table 2) were analyzed by RP-HPLC (for the crude samples, see Figure S1) and MS/HRMS (for crude/pure samples, see Table S1). In each library, the samples that maintained a dark coloration after

treatment with hydrogen sulfide were submitted to ICP analyses to determine their copper contents. As all the crude mixtures of the compounds from the focused library (Table 2) visually appeared to be free of copper, we randomly selected the crude compounds **C4B2A10**, **C4B3A6** and **C4B3B2**, which gave some response in the IR-A phosphorylation assay, and determined their copper contents.

Biology

Assays. The cell lines that were employed for the receptor binding studies and stimulation of autophosphorylation were the human IM-9 lymphocytes (for IR-A, purchased from ATCC) and mouse embryonic fibroblasts with a targeted disruption of IGF-1R that were stably transfected with either human IR-A (R^-/IR-A) or human IGF-1R (R^{+39}) and kindly provided by A. Belfiore (University of Magna Graecia, Catarzano, Italy) and R. Baserga (Thomas Jefferson University, Philadelphia, PA). The cells were grown and treated as previously described.[21]

Stock 1 mM solutions of the libraries and single compounds were prepared in 100 mM Hepes/NaOH buffer, pH 7.5 and the concentrations were determined based on quantitative ^{19}F NMR analyses as described previously.[10] The concentrations of the compounds from the focused library (**C4B2A10**, **C4B3A6**, **C4A10A10**, **C4A6A10**, **C4B3A10**, **C4A6A6**, **C4B2A6**, **C4B2B2**, **C4B3B2** and **C4B3B3**) were prepared with the HPLC purified products based on their molecular weights. The RP-HPLC-isolated fractions (**C4-1** and **C4-2**) were dissolved in the same buffer at 1 mg/mL (w/v) (because not enough material was available for ^{19}F NMR analysis), which should roughly correspond to 1 mM solutions of the single compounds (molecular weights ranging from 800 Da to 1,200 Da). As needed, the solutions were heated and sonicated to support solubility.

All libraries and single compounds were tested for binding to human IR-A (in the membranes of human IM-9 lymphocytes) and to human IGF-1R (in the membranes of mouse embryonic fibroblasts) at a single concentration (0.1 mM or 0.1 mg/mL) and at least three times. Eventually, 0.01 mM concentrations were checked. The binding assays were performed as recently described by Krizkova et al.[21]

Mouse fibroblasts (R^-/IR-A) and (R^{+39}) were stimulated with the libraries, single compounds and RP-HPLC-isolated fractions at concentrations of 0.1 mM or 0.1 mg/mL for 10 min in 24-well plates. The cells were lysed and immunoblotted onto a PVDF membrane, as described by Krizkova et al.[21] The membranes were probed with an anti-phospho-IGF-1R β-subunit (Tyr1131)

/IR β-subunit (Tyr1146) antibody (Cell Signaling Technology) to detect the extent of receptor autophosphorylation. The cells in the control wells were treated with either buffer alone or with 10 nM insulin (Sigma). The series of samples were tested four times using different batches of cells. The signal density generated by a sample was expressed as the contribution of phosphorylation relative to the signal from 10 nM insulin in the same experiment. The significance of an increase in the signal density generated by a particular sample (mean ± standard error of the mean (SEM), n = 4) compared with the control (unstimulated cells) was calculated using one-way analysis of variance.

Determination of the impact of copper. Copper(II) sulfate pentahydrate (2.5 mg, 10 μmol) was dissolved in 3 mL of 100 mM Hepes/NaOH buffer, pH 7.5. Gaseous hydrogen sulfide (H_2S) was blown at the surface of the solutions while stirring. The solution was allowed to stand for 30 minutes and completely turned black. After lyophilization, the black residue was redissolved (suspension) in MQ water (virtual copper concentration of 3 mM) and diluted ten-fold for the assays (final virtual copper concentration of 300 μM). This sample was tested alone or with insulin (at 10 nM) and did not show false positive or negative results (not shown).

ASSOCIATED CONTENT

Supporting Information

The Supporting Information is available free of charge on the ACS Publications website at DOI:

Syntheses of azides **A1-C10** and the scaffold **I**. Description of methods to remove copper. Figures showing RP-HPLC analyses of the sub-library **C4B7** and compounds **C4B7A1-C4B7A10**. Figure showing LC-MS analysis of **C4B7**. Table showing analytical data for selected sub-libraries and compounds. Figures showing biological activities of sub-libraries and single compounds. Figures showing HPLC traces of the compounds from the focused library. Tables showing crude yields of sub-libraries **C1-C10** and **C4B1-C4B10** and compounds **C4B7A1-C4B7A10**. Figures showing HPLC traces and mass spectra of the **C2** sub-library before and after the extraction with diethyl ether. Figure showing HPLC traces of the sub-library **C1** before and after treatment with hydrogen sulfide. Supplementary references. (PDF).

AUTHOR INFORMATION

Corresponding Author

*Phone: +420 220183-441. E-mail: jiracek@uochb.cas.cz

Authors' Contributions

BJ and JP contributed equally to this work; BJ, JP, VV and IS conceived and performed the experiments, analyzed the data and co-wrote the manuscript; MC, MC and LZ performed the experiments and analyzed the data; MB measured and analyzed the NMR spectra; JJ conceived the study, analyzed the data and co-wrote the manuscript. All authors have given their final approval to the final version of the manuscript.

Funding

This work was supported by the Grant Agency of the Czech Republic (grant 14-17305S, to J.J.), by the Academy of Sciences of the Czech Republic (Research Project RVO:6138963, support to the Institute of Organic Chemistry and Biochemistry and postdoctoral stipend to B.F.), by the Institute of Organic Chemistry and Biochemistry (IOCB) and the Czech Academy of Sciences (postdoctoral stipend to B.F.) and partially by the Medical Research Council (Grant MR/K000179/1).

Notes

The authors declare that there are no competing financial interests.

ACKNOWLEDGEMENTS

The authors would like to thank Dr. Stanislava Matějková for performing the ICP analyses.

ABBREVIATIONS

CuAAC, copper(I)-catalyzed azide–alkyne cycloaddition; ICP, inductively coupled plasma; IGF-1R, insulin-like growth factor 1 receptor; IR, insulin receptor; IR-A, isoform A of the insulin receptor.

REFERENCES

(1) Milroy, L. G., Grossmann, T. N., Hennig, S., Brunsveld, L., and Ottmann, C. Modulators of protein-protein interactions, *Chem. Rev.* **2014**, *114*, 4695-4748.

(2) Wells, J. A., and McClendon, C. L. Reaching for high-hanging fruit in drug discovery at protein-protein interfaces, *Nature* **2007**, *450*, 1001-1009.

(3) Robinson, J. A., DeMarco, S., Gombert, F., Moehle, K., and Obrecht, D. The design, structures and therapeutic potential of protein epitope mimetics, *Drug Discov. Today* **2008**, *13*, 944-951.

(4) Fletcher, S., and Hamilton, A. D. Protein surface recognition and proteomimetics: mimics of protein surface structure and function, *Curr. Opin. Chem. Biol.* **2005**, *9*, 632-638.

(5) Jones, S., and Thornton, J. M. Principles of protein-protein interactions, *Proc. Natl. Acad. Sci. U.S.A.* **1996**, *93*, 13-20.

(6) Lo Conte, L., Chothia, C., and Janin, J. The atomic structure of protein-protein recognition sites, *J. Mol. Biol.* **1999**, *285*, 2177-2198.

(7) Cunningham, B. C., and Wells, J. A. High-resolution epitope mapping of hgh-receptor interactions by alanine-scanning mutagenesis, *Science* **1989**, *244*, 1081-1085.

(8) Moreira, I. S., Fernandes, P. A., and Ramos, M. J. Hot spots-A review of the protein-protein interface determinant amino-acid residues, *Proteins* **2007**, *68*, 803-812.

(9) Beal, D. M., and Jones, L. H. Molecular scaffolds using multiple orthogonal conjugations: Applications in chemical biology and drug discovery, *Angew. Chem. Int. Edit.* **2012**, *51*, 6320-6326.

(10) Vanek, V., Picha, J., Fabre, B., Budesinsky, M., Lepsik, M., and Jiracek, J. The development of a versatile trifunctional scaffold for biological applications, *Eur. J. Org. Chem.* **2015**, 3689-3701.

(11) Ward, C. W., Menting, J. G., and Lawrence, M. C. The insulin receptor changes conformation in unforeseen ways on ligand binding: Sharpening the picture of insulin receptor activation, *Bioessays* **2013**, *35*, 945-954.

(12) Zakova, L., Barth, T., Jiracek, J., Barthova, J., and Zorad, S. Shortened insulin analogues: Marked changes in biological activity resulting from replacement of TyrB26 and N-methylation of peptide bonds in the C-terminus of the B-chain, *Biochemistry* **2004**, *43*, 2323-2331.

(13) Zakova, L., Brynda, J., Au-Alvarez, O., Dodson, E. J., Dodson, G. G., Whittingham, J. L., and Brzozowski, A. M. Toward the insulin-IGF-I intermediate structures: Functional and structural properties of the [Tyr(B25)NMePhe(B26)] insulin mutant, *Biochemistry* **2004**, *43*, 16293-16300.

(14) Zakova, L., Kazdova, L., Hanclova, I., Protivinska, E., Sanda, M., Budesinsky, M., and Jiracek, J. Insulin analogues with modifications at position B26. Divergence of binding affinity and biological activity, *Biochemistry* **2008**, *47*, 5858-5868.

(15) Jiracek, J., Zakova, L., Antolíková, E., Watson, C. J., Turkenburg, J. P., Dodson, G. G., and Brzozowski, A. M. Implications for the active form of human insulin based on the structural convergence of highly active hormone analogues., *Proc. Natl. Acad. Sci. U.S.A.* **2010**, *107*, 1966-1970.

(16) Antolikova, E., Zakova, L., Turkenburg, J. P., Watson, C. J., Hanclova, I., Sanda, M., Cooper, A., Kraus, T., Brzozowski, A. M., and Jiracek, J. Non-equivalent role of inter- and intramolecular hydrogen bonds in the insulin dimer interface, *J. Biol. Chem.* **2011**, *286*, 36968-36977.

(17) Zakova, L., Kletvikova, E., Veverka, V., Lepsik, M., Watson, C. J., Turkenburg, J. P., Jiracek, J., and Brzozowski, A. M. Structural Integrity of the B24 Site in Human Insulin Is Important for Hormone Functionality, *J. Biol. Chem.* **2013**, *288*, 10230-10240.

(18) Krizkova, K., Veverka, V., Maletinska, L., Hexnerova, R., Brzozowski, A. M., Jiracek, J., and Zakova, L. Structural and functional study of the GlnB22-insulin mutant responsible for maturity-onset diabetes of the young, *Plos One* **2014**, *9*, e112883.

(19) Kosinova, L., Veverka, V., Novotna, P., Collinsova, M., Urbanova, M., Moody, N. R., Turkenburg, J. P., Jiracek, J., Brzozowski, A. M., and Zakova, L. Insight into the structural and biological relevance of the T/R transition of the N-terminus of the B-chain in human insulin, *Biochemistry* **2014**, *53*, 3392-3402.

(20) Vikova, J., Collinsova, M., Kletvikova, E., Budesinsky, M., Kaplan, V., Zakova, L., Veverka, V., Hexnerova, R., Avino, R. J. T., Strakova, J., Selicharova, I., Vanek, V., Wright, D. W., Watson, C. J., Turkenburg, J. P., Brzozowski, A. M., and Jiracek, J. Rational steering of insulin binding specificity by intra-chain chemical crosslinking, *Scientific Reports* **2016**, *6, 19431*.

(21) Krizkova, K., Chrudinova, M., Povalova, A., Selicharova, I., Collinsova, M., Vanek, V., Brzozowski, A. M., Jiracek, J., and Zakova, L. Insulin-insulin-like growth factors hybrids as molecular probes of hormone:receptor binding specificity, *Biochemistry* **2016**, *55*, 2903-2913.

(22) Menting, J. G., Whittaker, J., Margetts, M. B., Whittaker, L. J., Kong, G. K. W., Smith, B. J., Watson, C. J., Zakova, L., Kletvikova, E., Jiracek, J., Chan, S. J., Steiner, D. F., Dodson, G. G., Brzozowski, A. M., Weiss, M. A., Ward, C. W., and Lawrence, M. C. How insulin engages its primary binding site on the insulin receptor, *Nature* **2013**, *493,* 241-245.

(23) Menting, J. G., Yang, Y. W., Chan, S. J., Phillips, N. B., Smith, B. J., Whittaker, J., Wickramasinghe, N. P., Whittaker, L. J., Pandyarajan, V., Wan, Z. L., Yadav, S. P., Carroll, J. M., Strokes, N., Roberts, C. T., Ismail-Beigi, F., Milewski, W., Steiner, D. F., Chauhan, V. S., Ward, C. W., Weiss, M. A., and Lawrence, M. C. Protective hinge in insulin opens to enable its receptor engagement, *Proc. Natl. Acad. Sci. U.S.A.* **2014**, *111*, E3395-E3404.

(24) Zakova, L., Kletvikova, E., Lepsik, M., Collinsova, M., Watson, C. J., Turkenburg, J. P., Jiracek, J., and Brzozowski, A. M. Human insulin analogues modified at the B26 site reveal a hormone conformation that is undetected in the receptor complex, *Acta Crystallogr. D* **2014**, *70*, 2765-2774.

(25) De Meyts, P. Insulin/receptor binding: The last piece of the puzzle? *Bioessays* **2015**, *37*, 389-397.

(26) Zhang, B., Salituro, G., Szalkowski, D., Li, Z. H., Zhang, Y., Royo, I., Vilella, D., Diez, M. T., Pelaez, F., Ruby, C., Kendall, R. L., Mao, X. Z., Griffin, P., Calaycay, J., Zierath, J. R., Heck, J. V., Smith, R. G., and Moller, D. E. Discovery of a small molecule insulin mimetic with antidiabetic activity in mice, *Science* **1999**, *284*, 974-977.

(27) Schlein, M., Ludvigsen, S., Olsen, H. B., Andersen, A. S., Danielsen, G. M., and Kaarsholm, N. C. Properties of small molecules affecting insulin receptor function, *Biochemistry* **2001**, *40*, 13520-13528.

(28) Nakamura, T., Takahashi, H., Takahashi, M., Shimba, N., Suzuki, E., and Shimada, I. Direct determination of the insulin-insulin receptor interface using transferred cross-saturation experiments, *J. Med. Chem.* **2010**, *53*, 1917-1922.

(29) Tan, C., Wei, L. H., Ottensmeyer, F. P., Goldfine, I., Maddux, B. A., Yip, C. C., Batey, R. A., and Kotra, L. P. Structure-based de novo design of ligands using a three-dimensional model of the insulin receptor, *Bioorg. Med. Chem. Lett.* **2004**, *14*, 1407-1410.

(30) Li, Y. S., Kim, J., Li, J., Liu, F., Liu, X. Q., Himmeldirk, K., Ren, Y. L., Wagner, T. E., and Chen, X. Z. Natural anti-diabetic compound 1,2,3,4,6-penta-O-galloyl-D-glucopyranose binds to insulin receptor and activates insulin-mediated glucose transport signaling pathway, *Biochem. Biophys. Res. Commun.* **2005**, *336*, 430-437.

(31) Pillutla, R. C., Hsiao, K. C., Beasley, J. R., Brandt, J., Ostergaard, S., Hansen, P. H., Spetzler, J. C., Danielsen, G. M., Andersen, A. S., Brissette, R. E., Lennick, M., Fletcher, P. W., Blume, A. J., Schaffer, L., and Goldstein, N. I. Peptides identify the critical hotspots involved in the biological activation of the insulin receptor, *J. Biol. Chem.* **2002**, *277*, 22590-22594.

(32) Schaffer, L., Brissette, R. E., Spetzler, J. C., Pillutla, R. C., Ostergaard, S., Lennick, M., Brandt, J., Fletcher, P. W., Danielsen, G. M., Hsiao, K. C., Andersen, A. S., Dedova, O., Ribel, U., Hoeg-Jensen, T., Hansen, P. H., Blume, A. J., Markussen, J., and Goldstein, N. I. Assembly of high-affinity insulin receptor agonists and antagonists from peptide building blocks, *Proc. Natl. Acad. Sci. U.S.A.* **2003**, *100*, 4435-4439.

(33) Jensen, M., Hansen, B., De Meyts, P., Schaffer, L., and Urso, B. Activation of the insulin receptor by insulin and a synthetic peptide leads to divergent metabolic and mitogenic signaling and responses, *J. Biol. Chem.* **2007**, *282*, 35179-35186.

(34) Yunn, N. O., Koh, A., Han, S., Lim, J. H., Park, S., Lee, J., Kim, E., Jang, S. K., Berggren, P. O., and Ryu, S. H. Agonistic aptamer to the insulin receptor leads to biased signaling and functional selectivity through allosteric modulation, *Nucleic Acids Res.* **2015**, *43*, 7688-7701.

(35) Furka, A., Sebestyen, F., Asgedom, M., and Dibo, G. General-method for rapid synthesis of multicomponent peptide mixtures, *Int. J. Pept. Prot. Res.* **1991**, *37*, 487-493.

(36) Houghten, R. A., Pinilla, C., Blondelle, S. E., Appel, J. R., Dooley, C. T., and Cuervo, J. H. Generation and Use of Synthetic Peptide Combinatorial Libraries for Basic Research and Drug Discovery, *Nature* **1991**, *354*, 84-86.

(37) Lam, K. S., Salmon, S. E., Hersh, E. M., Hruby, V. J., Kazmierski, W. M., and Knapp, R. J. A New Type of Synthetic Peptide Library for Identifying Ligand-Binding Activity, *Nature* **1991**, *354*, 82-84.

(38) Garcia-Martin, F., Quintanar-Audelo, M., Garcia-Ramos, Y., Cruz, L. J., Gravel, C., Furic, R., Cote, S., Tulla-Puche, J., and Albericio, F. ChemMatrix, a poly(ethylene

glycol)-based support for the solid-phase synthesis of complex peptides, *J. Comb. Chem.* **2006**, *8*, 213-220.

(39) Garcia-Ramos, Y., Paradis-Bas, M., Tulla-Puche, J., and Albericio, F. ChemMatrix(R) for complex peptides and combinatorial chemistry, *J. Pept. Sci.* **2010**, *16*, 675-678.

(40) Fabre, B., Picha, J., Vanek, V., Budesinsky, M., and Jiracek, J. A CuAAC-hydrazone-CuAAC Trifunctional scaffold for the solid-phase synthesis of trimodal compounds: possibilities and limitations, *Molecules* **2015**, *20*, 19310-19329.

(41) Ramage, R., Irving, S. L., and Mcinnes, C. Design of a versatile linker for solid-phase peptide-synthesis - synthesis of C-terminal primary secondary amides and hydrazides, *Tetrahedron Lett.* **1993**, *34*, 6599-6602.

(42) Valverde, I. E., Delmas, A. F., and Aucagne, V. Click a la carte: robust semi-orthogonal alkyne protecting groups for multiple successive azide/alkyne cycloadditions, *Tetrahedron* **2009**, *65*, 7597-7602.

(43) Werkhoven, P. R., van de Langemheen, H., van der Wal, S., Kruijtzer, J. A. W., and Liskamp, R. M. J. Versatile convergent synthesis of a three peptide loop containing protein mimic of whooping cough pertactin by successive Cu(I)-catalyzed azide alkyne cycloaddition on an orthogonal alkyne functionalized TAC-scaffold, *J. Pept. Sci.* **2014**, *20*, 235-239.

(44) Werkhoven, P. R., Elwakiel, M., Meuleman, T. J., van Ufford, H. C. Q., Kruijtzer, J. A. W., and Liskamp, R. M. J. Molecular construction of HIV-gp120 discontinuous epitope mimics by assembly of cyclic peptides on an orthogonal alkyne functionalized TAC-scaffold, *Org. Biomol. Chem*. **2016**, *14*, 701-710.

(45) Castro, V., Rodriguez, H., and Abericio, F. CuAAC: An Efficient Click Chemistry Reaction on Solid Phase, *ACS Comb. Sci.* **2016**, *18*, 1-14.

(46) Mayer, J. P., Zhang, F., and DiMarchi, R. D. Insulin Structure and Function, *Biopolymers* **2007**, *88*, 687-713.

Table of Contents Graphics